Pointers toward the Occurrence of C−F···F−C Interaction: Experimental Charge Density Analysis of 1-(4-Fluorophenyl)-3,6,6-trimethyl-2-phenyl-1,5,6,7-tetrahydro-4*H*-indol-4-one and 1-(4-Fluorophenyl)-6-methoxy-2-phenyl-1,2,3,4-tetrahydroisoquinoline

Deepak Chopra,[†] T. S. Cameron,[‡] Joseph D. Ferrara,[§] and Tayur N. Guru Row*[,†]

Solid State and Structural Chemistry Unit, Indian Institute of Science, Bangalore 560012, India, Department of Chemistry, Dalhousie University, Halifax H.S., Canada B3H 4J3, and Rigaku/MSC, The Woodlands, Texas 77381

Received: April 25, 2006; In Final Form: June 15, 2006

A charge density study of crystalline 1-(4-fluorophenyl)-3,6,6-trimethyl-2-phenyl-1,5,6,7-tetrahydro-4*H*-indol-4-one (**A**) and 1-(4-fluorophenyl)-6-methoxy-2-phenyl-1,2,3,4-tetrahydroisoquinoline (**B**) has been carried out using high-resolution X-ray diffraction data collected at 113(2) K. Weak intermolecular interactions of the type C−H···O, C−H···π, and π···π hold the molecules together in the crystal lattice along with interactions of the type C−H···F and unusual C−F···F−C examined via charge density analysis. The topological features are evaluated in terms of Bader's theory of atoms in molecules through the first four criteria of Koch and Popelier. The C−F···F−C contact is observed to be across the center of symmetry in **B** and not in **A**, and further, this interaction appears to possess a certain correlation with the electron density properties at the critical point which suggests that such an interaction fits into the hierarchy of weak interactions.

Introduction

Charge density analysis has gained immense importance in recent years, particularly because such studies allow one to observe and quantify hydrogen bonding beyond the criteria of mere geometry.[1] The theory of "atoms in molecules"[2,3] has not only provided a new pathway to evaluate derived properties on the basis of charge density measurements but also allows for comparison with theoretical estimates of such densities. Extensive studies related to crystal engineering aspects of C−H···O and C−H···π interactions have revealed the geometrical restraints of these contacts, which occur as both intra- and intermolecular interactions.[4−8] Several recent high-resolution X-ray diffraction studies[9−11] to unravel the nature of C(aryl)−H···π interactions in terms of electron densities, bond critical points, and Laplacian have clearly established that the interaction lines are curved and are almost perpendicular to the aromatic rings. In addition, there has been considerable focus and attention drawn to understand the nature of short contacts involving halogens of the type C−X···X (where X = F, Cl, Br, I) and contacts of the type C−X···O, C−X···N, and C−X···H (where X = C, N, O).[12−18] Such contacts have been known for sometime in crystallographic literature, wherein a short contact between two atoms, A and B, signifies that the distance A···B is less than the sum of the van der Waals radii.[18] An analysis of the topological properties of the electron density revealing weak closed-shell bonding interactions between chlorine atoms belonging to neighboring molecules in solid molecular chlorine crystals has been described recently.[19]

However, fluorine, particularly when it is covalently bonded continues to be a case of concern,[20] ascribed because of its high electronegativity. The highly polar C−F bond, the so-called organic fluorine, has thus been a subject of interest and reports on charge density analysis in fluorine containing compounds are hence of relevance.[21−26] Recently, Bach, Lentz, and Luger[27] have described weak intermolecular C−F···O and C−F···F−C bonding interactions in an ED study performed on pentafluorobenzoic acid at 110 K using multipolar refinement. The discrepancies between the experimental and theoretical Laplacian at the bond critical points of the C−F are highlighted, and the energetic disadvantage of F···F′ interaction has been examined. Bianchi, Forni, and Pilati[28] have performed experimental charge density calculations in the complex of (*E*)-1,2-bis(4-pyridyl) ethylene with 1,4-diiodotetrafluorobenzene at 90 K and highlighted that F···F, C···F, and C···C intermolecular interactions are significantly detectable and reinforce the crystal packing. Indeed, the importance of interactions such as F···F, C−H···F, and C−F···π to provide stability to form molecular assemblies in the absence of any other strong intermolecular forces such as hydrogen bonds has been established[29] by careful structural studies. In all such studies and especially in the study of the isomers of tetrafluorophthalonitrile,[30] the closed-shell nature of the C−F bond is obvious. However, the covalent nature of the bond is seen in the topological analysis. The appearance of F···F contacts as a consequence is indeed real and is not due to any unexpected features of the associated potential energy surfaces.[30] We have been interested in the classification of weak hydrogen bonds against van der Waals contacts and have clearly established the existence of a "region of overlap" which delineates the two types of intermolecular interactions.[1]

It has been demonstrated that an accurate experimental measurement and analysis of charge density in a molecular crystal can be obtained from high-resolution X-ray diffraction data at low temperatures.[31] The nature of chemical interactions can be evaluated in terms of the deformation densities.[32,33] The commonly used algorithm for this purpose is the Hansen−

* To whom correspondence should be addressed. Phone: +91-80-22932796, +91-80-22932336. Fax: +91-80-23601310. E-mail: ssctng@sscu.iisc.ernet.in.
[†] Indian Institute of Science.
[‡] Dalhousie University.
[§] Rigaku/MSC.

10.1021/jp0625309 CCC: $33.50
Published on Web 08/11/2006

SCHEME 1: Molecular Structure of the Two Molecules

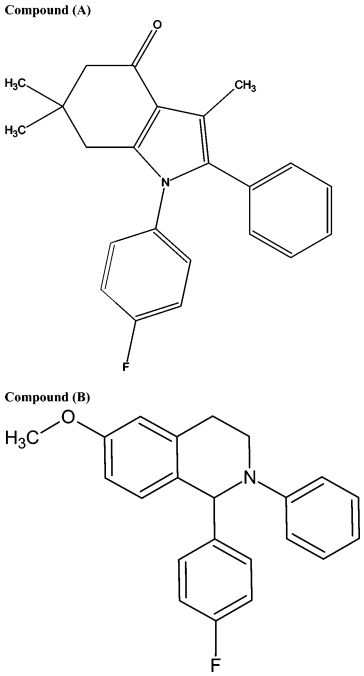

Coppens formalism[34] in which the individual atomic densities are divided into three components, the core, the spherical expansion and contraction term (κ) in the valence shell, and the valence deformation in terms of density normalized spherical harmonics ($d_{lm\pm}$), together with the corresponding radial expansion and contraction (κ') of the valence shell as given below

$$\rho_{at}(r) = P_c\rho_{core}(\mathbf{r}) + P_v\kappa^3\rho_{valenc}(\kappa\mathbf{r}) + \sum_{l=0}^{l_{max}} \kappa'^3 R_l(\kappa'\mathbf{r}) \sum_{m=0}^{l} P_{lm\pm} d_{lm\pm}(\vartheta,\varphi)$$

The electron density in the crystal is modeled on the basis of this $\rho(\mathbf{r})$ as a sum of atom centered charge distributions

$$\rho(\mathbf{r}) = \sum_j \rho_j(\mathbf{r}_j)$$

The derived experimental electron density can then be subjected to Bader's quantum theory of atoms in molecules (AIM)[2,3] which allows for the interpretation of detailed topological analysis which manifest as local maxima at the positions of the nuclei. In general, the theory of AIM provides a methodology for the identification of a bond between any two atoms in a molecule. This analysis is based on the identification of critical points, classified using the Hessian matrix of the electron density.[31] The bond critical points (BCPs) lie along the bond path with the gradient of the electron density, $\Delta\rho_b(\mathbf{r}) = 0$. The line of the highest electron density, referred to as the interaction line, with its length, R_{ij}, defines the "bond path" between any two atoms (not the same as interatomic vector). The second derivative of the electron density, the *Laplacian* $\nabla^2\rho_b(\mathbf{r})$ ($=\sum_{i=1}^{3}\lambda_i$, λ_i are the curvatures of a bond at the BCP), is expected to provide details of the chemical nature of the molecules, for example, $\nabla^2\rho_b(\mathbf{r}) < 0$ represents shared interactions, while $\nabla^2\rho_b(\mathbf{r}) > 0$ represents closed-shell interactions. The bond paths, interaction lines, and Laplacian values together represent the topology of the charge density distribution in a given molecule.

TABLE 1: Experimental X-ray Data

compound	**A**	**B**
formula weight	347.42	333.4
space group	$P4_2/n$	$C2/c$
temperature (K)	113(2)	113(2)
unit cell dimensions (Å):		
a	18.080(3)	16.414(9)
b	18.080(3)	9.300(6)
c	11.367(2)	23.435(14)
α (deg)	90	90
β (deg)	90	107.694(8)
γ (deg)	90	90
V (Å^3)	3715.8(9)	3408.2(9)
Z	8	8
D_c (g cm^{-1})	1.242	1.300
F(000)	1472	1407.8
absorption coeff (mm^{-1})	0.082	0.087
radiation	MoK$_\alpha$	MoK$_\alpha$
(sin θ/λ)$_{max}$ (Å^{-1})	1.1	1.1
reflections no. (unique)	12931	19037
$R(F^2)$	0.0465	0.0494
$R_w(F^2)$	0.0562	0.0612
S	4.0672	2.9318
N_{obsd}/N_{par}	18.06	21.56
range of residual density in asymmetric units (e/Å^3)	0.355/−0.417	0.170/−0.191

The topological analysis however does not specify the character of the bond but only indicates the existence of a bond. To characterize a bond in terms of its chemical concepts such as bond order, ionicity, conjugation, and hydrogen bonding, the properties evaluated at the BCPs become crucial. Koch and

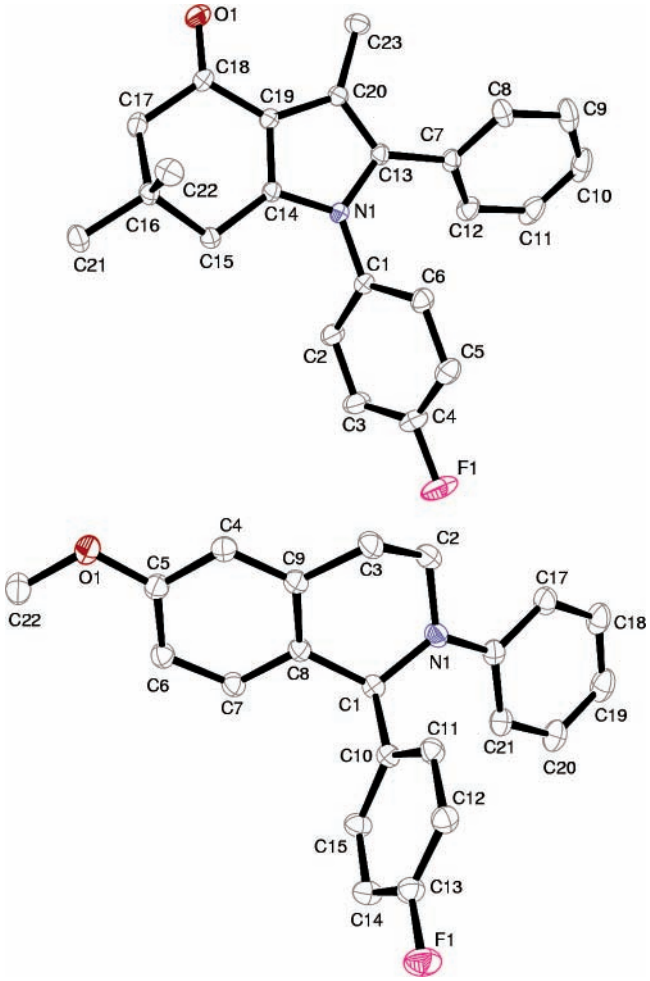

Figure 1. ORTEP of **A** and **B** drawn with 50% ellipsoidal probability with the relevant atom numbering.

TABLE 2: Intramolecular Bond Critical Points for the Compounds, Bond Ellipticity, $\epsilon = (\lambda_1/\lambda_2 - 1)$

bond (**A**−**B**)	ρ_b	$\nabla^2\rho_b$	R_{ij}	$d1$(**A**−CP)	$d2$(**B**−CP)	λ_1	λ_2	λ_3	ϵ
				A					
F(1)−C(4)	1.789(18)	−23.05(8)	1.3540	0.8633	0.490	−15.2	−13.6	5.8	0.12
O(1)−C(18)	2.691(24)	−24.38(7)	1.2354	0.8158	0.4196	−31.3	−24.5	31.4	0.28
N(1)−C(1)	1.802(16)	−18.74(7)	1.4250	0.9825	0.4425	−17.3	−15.6	14.2	0.11
N(1)−C(13)	1.778 (18)	−5.22(8)	1.4113	0.9836	0.4276	−16.4	−12.4	23.6	0.33
N(1)−C(14)	1.931(20)	−6.95(7)	1.3626	0.9427	0.4199	−18.2	−17.9	29.1	0.02
C(1)−C(2)	2.198(19)	−25.75(2)	1.3951	0.7421	0.6530	−19.1	−15.1	8.4	0.27
C(1)−C(6)	2.171(20)	−24.57(2)	1.3953	0.7244	0.6709	−18.6	−14.5	8.5	0.28
C(2)−C(3)	2.162(15)	−24.36(3)	1.3916	0.6846	0.7070	−18.1	−14.5	8.3	0.25
C(3)−C(4)	2.251(21)	−26.29(3)	1.3827	0.6319	0.7508	−19.6	−14.3	7.5	0.36
C(4)−C(5)	2.191(24)	−26.12(3)	1.3881	0.8101	0.5780	−18.5	−13.3	5.6	0.39
C(5)−C(6)	2.062(18)	−23.922(2)	1.3945	0.7792	0.6152	−16.9	−13.4	6.5	0.26
C(7)−C(8)	2.168(19)	−24.33(3)	1.3985	0.6837	0.7149	−18.7	−14.2	8.6	0.32
C(7)−C(12)	2.108(24)	−23.30(3)	1.4023	0.7183	0.6840	−18.1	−13.8	8.6	0.31
C(7)−C(13)	1.806(21)	−16.81(3)	1.4703	0.7131	0.7572	−13.9	−12.1	9.2	0.16
C(8)−C(9)	2.105(10)	−22.84(4)	1.3928	0.7172	0.6757	−17.2	−13.6	8.0	0.26
C(9)−C(10)	2.129(11)	−22.26(4)	1.3925	0.7087	0.6838	−17.1	−13.9	8.8	0.23
C(10)−C(11)	2.240(25)	−27.073)	1.3945	0.6310	0.7635	−19.6	−15.6	8.1	0.26
C(11)−C(12)	2.132(25)	−25.43(3)	1.3882	0.7184	0.6698	−18.5	−14.4	7.5	0.29
C(13)−C(20)	2.152(18)	−22.88(3)	1.3831	0.7436	0.6395	−18.1	−12.9	8.2	0.40
C(14)−C(15)	1.773(25)	−18.17(5)	1.4899	0.8261	0.6638	−13.9	−11.8	7.5	0.18
C(14)−C(19)	2.179(16)	−24.18(6)	1.3909	0.7481	0.6428	−18.3	−14.0	8.2	0.31
C(15)−C(16)	1.599(27)	−12.88(5)	1.5411	0.7692	0.7718	−10.8	−10.7	8.6	0.00
C(16)−C(17)	1.636(24)	−12.25(5)	1.5421	0.7884	0.7537	−11.1	−10.7	9.5	0.04
C(16)−C(21)	1.662(28)	−15.84(6)	1.5280	0.7874	0.7406	−12.9	−11.3	8.3	0.14
C(16)−C(22)	1.650(14)	−13.39(4)	1.5289	0.8125	0.7164	−11.2	−10.9	8.7	0.02
C(17)−C(18)	1.737(17)	−14.48(4)	1.5217	0.7417	0.7800	−12.9	−11.6	9.9	0.11
C(18)−C(19)	1.911(16)	−18.60(4)	1.4459	0.7568	0.6891	−15.6	−12.1	9.1	0.28
C(19)−C(20)	1.937(18)	−18.24(3)	1.4392	0.7271	0.7121	−14.9	−12.4	9.2	0.21
C(20)−C(23)	1.755(9)	−16.74(3)	1.4936	0.7650	0.7286	−13.5	−11.9	8.7	0.13
				B					
F(1)−C(13)	1.607(16)	−7.21(8)	1.3589	0.9203	0.4386	−12.1	−10.7	15.6	0.12
O(1)−C(5)	1.636 (20)	−8.51(11)	1.3719	0.9290	0.4430	−12.7	−11.4	15.6	0.11
O(1)−C(22)	1.604 (32)	−20.92(15)	1.4215	0.9594	0.4621	−14.9	−11.6	5.7	0.28
N(1)−C(1)	1.630(17)	−16.42(6)	1.4680	0.8798	0.5882	−11.2	−9.7	4.5	0.15
N(1)−C(16)	1.838(19)	−14.27(10)	1.3931	0.9535	0.4397	−15.1	−13.1	13.9	0.15
C(1)−C(8)	1.561(10)	−12.53(2)	1.5237	0.7651	0.7586	−9.7	−8.7	5.9	0.12
C(1)−C(10)	1.613(11)	−12.57(3)	1.5342	0.7209	0.8133	−9.8	−9.2	6.4	0.07
C(2)−C(3)	1.559(13)	−11.26(3)	1.5242	0.7614	0.7628	−9.8	−8.4	6.9	0.16
C(3)−C(9)	1.695(13)	−14.33(3)	1.4975	0.7253	0.7722	−10.9	−9.6	6.2	0.15
C(4)−C(5)	2.003(13)	−24.32(4)	1.3993	0.6336	0.7657	−15.3	−11.5	2.5	0.33
C(4)−C(9)	1.954(12)	−21.96(3)	1.3951	0.6687	0.7264	−14.3	−10.7	3.0	0.33
C(5)−C(6)	1.923(12)	−20.79(3)	1.3983	0.7207	0.6776	−13.6	−10.5	3.3	0.29
C(6)−C(7)	1.925(11)	−20.53(4)	1.3969	0.6874	0.7096	−13.7	−10.3	3.5	0.33
C(7)−C(8)	2.024(11)	−22.81(3)	1.3949	0.6792	0.7157	−14.9	−11.4	3.5	0.32
C(8)−C(9)	2.009(11)	−21.26(3)	1.4005	0.6983	0.7022	−14.2	−10.8	3.8	0.31
C(10)−C(11)	2.105(10)	−23.99(3)	1.3970	0.6978	0.6993	−15.5	−12.5	3.9	0.24
C(10)−C(15)	1.937 (11)	−20.96(3)	1.3995	0.7187	0.6809	−13.5	−10.9	3.4	0.24
C(11)−C(12)	1.976(11)	−21.88(3)	1.3988	0.7013	0.6975	−14.2	−11.2	3.6	0.27
C(12)−C(13)	2.043(12)	−23.63(3)	1.3866	0.6740	0.7127	−15.1	−12.0	3.5	0.26
C(14−C(15))	1.962(12)	−21.30 (3)	1.3969	0.6834	0.7135	−14.1	−11.2	3.9	0.26
C(16)−C(17)	1.967 (12)	−22.24(4)	1.4130	0.7811	0.6319	−14.2	−10.8	2.8	0.31
C(17)−C(18)	2.014(13)	−23.66(3)	1.3928	0.6767	0.7161	−14.9	−11.9	3.1	0.25
C(19)−C(20)	1.929(16)	−23.13(6)	1.3971	0.7942	0.6029	−13.9	−10.7	1.5	0.30
C(20)−C(21)	1.954(12)	−21.84(3)	1.3936	0.6627	0.7309	−13.9	−10.9	3.0	0.28

Popelier have proposed eight criteria to establish hydrogen bonding in particular, which allows a hydrogen bond to be distinguished from a van der Waals interaction.[35,36] Among these eight criteria, the first four are sufficient, with the fourth being *necessary and sufficient* to fully describe a hydrogen bond. The **first** condition is the existence of a BCP between a donor atom and an acceptor atom linked via a bond path. The **second** condition is the presence of charge density evaluated at the BCP and its relationship with the overall hydrogen bond energy. It is possible to relate the charge density parameters at the BCP to the local energy density ($E(r_{CP})$) of the electrons by evaluating the local electronic kinetic energy density ($G(r_{CP})$) and the local potential energy density ($V(r_{CP})$) using the equations[2,37,38]

$$G(r_{CP}) = ({}^3/_{10})(3\pi^2)^{2/3}\rho^{5/3}(r_{CP}) + ({}^1/_6)\nabla^2\rho(r_{CP}) \quad (1)$$

$$V(r_{CP}) = ({}^1/_4)\nabla^2\rho(r_{CP}) - 2G(r_{CP}) \quad (2)$$

$$E(r_{CP}) = G(r_{CP}) + V(r_{CP}) \quad (3)$$

The **third** condition refers to the value of the Laplacian at the BCP. The calculated values of $\nabla^2\rho_b(\mathbf{r})$ should be positive and should correlate with the interaction energy. The value of $\nabla^2\rho_b(\mathbf{r})$ should also agree with the range of values found so far in the literature. The **fourth** condition deals with the mutual

TABLE 3: Intermolecular Bond Critical Points and the Parameters Characterizing the Interactions (The Symmetry Codes Are Given in the Second Row under Each Interaction)

interaction	R_{ij}	$\Delta r_D - \Delta r_A$	$\Delta r_D + \Delta r_A$	ρ_b	$\nabla^2\rho_b$	$G(r_{CP})$	$V(r_{CP})$
			A				
C3−X6_C(6)	3.6989	0.2105	−0.1589	0.026	0.268	10.15	−7.02
$(y,-x+1/2+1,-z+1/2)$							
C3−X5_C(11)	3.7079	0.0193	−0.2047	0.026	0.261	9.92	−6.91
$(-x+1,-y+2,-z+1)$							
C5−X4_C(23)	3.7790	0.0014	−0.315	0.025	0.261	9.84	−6.74
$y-1/2,-x+1,+z+1/2$							
C9−X3_C(9)	3.6250	0.2206	−0.085	0.038	0.416	16.18	−11.76
$(-x+1/2,y+1/2+1,+z)$							
C9−X2_C(19)	3.6600	0.1813	−0.1201	0.030	0.307	11.79	−8.37
$(-y+1,+x+1/2,+z+1/2)$							
C9−X2_C(20)	3.6658	0.3434	−0.1258	0.035	0.382	14.75	−10.57
$(-y+1,+x+1/2,+z+1/2)$							
C10−X4_C(23)	3.8539	0.0613	−0.3839	0.026	0.265	10.05	−6.97
$(y-1/2,-x+1,+z+1/2)$							
C14−X5_C(17)	3.8270	0.0108	−0.357	0.026	0.268	10.15	−7.02
$(-x+1,-y+2,-z)$							
C21−X6_C(22)	3.6841	0.0479	−0.2841	0.027	0.290	10.96	−7.56
$(y,-x+1/2+1,-z-1/2)$							
C1−X8_H(2)	3.6112	0.453	−0.6412	0.009	0.153	5.275	−2.97
$-y+1/2+1,+x,-z+1/2$							
C3−X5_H(8)	3.0994	0.2591	−0.1293	0.020	0.276	9.954	−6.24
$-x+1,-y+2,-z+1$							
C5−X8_H(10)	3.3540	0.2348	−0.384	0.016	0.240	8.505	−5.12
$-y+1/2+1,+x,-z+1/2$							
C5−X8_H(11)	3.318	0.2813	−0.3481	0.015	0.334	11.55	−6.55
$-y+1/2+1,+x,-z+1/2$							
C5−X8_H(15)	3.8243	0.1961	−0.8533	0.005	0.107	3.617	−1.93
$-y+1/2+1,+x,-z+1/2$							
C6−X8_H(2)	3.0982	0.0737	−0.1283	0.020	0.247	8.996	−5.76
$-y+1/2+1,+x,-z+1/2$							
C6−X4_H(21)	3.7266	0.0748	−0.7566	0.010	0.123	4.327	−2.56
$y-1/2,-x+1,+z+1/2$							
C8−X3_H(5)	3.4122	0.3710	−0.4422	0.024	0.310	11.375	−7.39
$-x+1/2,-y+1/2+1,+z$							
C9−X3_H(6)	2.9822	0.0767	−0.0123	0.035	0.435	16.498	−11.45
$-x+1/2,-y+1/2+1,+z$							
C10−X2_H(4)	3.7469	0.3899	−0.7769	0.007	0.116	3.977	−2.21
$-y+1,+x+1/2,+z+1/2$							
C10−X4_H(21)	2.9886	0.2549	−0.0187	0.028	0.463	16.761	−10.58
$y-1/2,-x+1,+z+1/2$							
C10−X4_H(22)	3.6291	0.0491	−0.6591	0.010	0.122	4.294	−2.54
$y-1/2,-x+1,+z+1/2$							
C11−X5_H(1)	3.5630	0.2338	−0.6110	0.008	0.147	5.037	−2.79
$-x+1,-y+2,-z+1$							
C11−X5_H(2)	3.3347	0.0941	−0.3639	0.015	0.182	6.530	−4.04
$-x+1,-y+2,-z+1$							
C11−X1_H(13)	3.1096	0.2392	−0.1351	0.022	0.344	12.344	−7.65
$x,+y,+z+1$							
C13−X4_H(7)	3.2772	0.1616	−0.3022	0.019	0.244	8.829	−5.57
$y-1/2,-x+1,+z-1/2$							
C14−X5_H(12)	2.8332	0.2739	0.1377	0.025	0.502	17.796	−10.72
$-x+1,-y+2,-z$							
C15−X8_H(2)	3.6107	0.5629	−0.7107	0.011	0.179	6.222	−3.56
$-y+1/2+1,+x,-z+1/2$							
C15−X5_H(20)	3.8154	0.5934	−0.9154	0.009	0.148	5.11	−2.89
$-x+1,-y+2,-z$							
C17−X5_H(9)	3.5781	0.4053	−0.6781	0.007	0.115	3.944	−2.19
$-x+1,-y+2,-z$							
C19−X5_H(11)	3.0462	0.1988	0.0762	0.033	0.369	14.119	−9.96
$-x+1,-y+2,-z$							
C21−X6_H(17)	3.1685	0.1148	−0.2684	0.024	0.309	11.342	−7.38
$y,-x+1/2+1,-z-1/2$							
C21−X6_H(18)	3.1638	0.2287	−0.2637	0.025	0.337	12.347	−8.00
$y,-x+1/2+1,-z-1/2$							
C21−X5_H(20)	3.6025	0.4303	−0.7017	0.013	0.215	7.51	−4.37
$-x+1,-y+2,-z$							
C22−X8_H(16)	3.4443	0.3711	−0.5443	0.021	0.282	10.223	−6.48
$-y+1/2+1,+x,-z-1/2$							
C23−X2_H(18)	3.1358	0.3466	−0.2358	0.031	0.453	16.702	−10.96
$-y+1,+x+1/2,+z+1/2$							

TABLE 3 (Continued)

interaction	R_{ij}	$\Delta r_D - \Delta r_A$	$\Delta r_D + \Delta r_A$	ρ_b	$\nabla^2\rho_b$	$G(r_{CP})$	$V(r_{CP})$
F1−X6_C(22) $y,-x+1/2+1,-z+1/2$	3.5946	0.4914	0.2054	0.018	0.244	8.762	−5.44
F1−X6_H(14) $y,-x+1/2+1,-z+1/2$	3.1721	−0.5037	−0.4721	0.034	0.556	20.394	−13.24
F1−X1_H(16) $x,+y,+z+1$	2.7946	0.0961	−0.0945	0.018	0.314	11.074	−6.59
F1−X6_H(17) $y,-x+1/2+1,-z+1/2$	2.5381	0.0217	+0.1619	0.044	0.697	26.141	−17.75
F1−X3_F(1) $-x+1/2+1,y+1/2+1,+z$	2.8091	0.0073	+0.1909	0.049	1.030	37.752	−24.48
O1−X5_C(2) $-x+1,-y+2,-z$	3.3511	0.1425	−0.1911	0.036	0.459	17.393	−12.05
O1−X2_C(6) $-y+1,+x+1/2,+z-1/2$	3.4192	0.1614	−0.2492	0.028	0.389	14.317	−9.36
O1−X1_C(10) $x,+y,+z-1$	3.5083	0.2895	−0.3383	0.019	0.230	8.366	−5.34
O1−X1_C(11) $x,+y,+z-1$	3.5065	0.2834	−0.3366	0.024	0.288	10.648	−7.03
O1−X5_H(1) $-x+1,-y+2,-z$	2.2914	0.3986	0.3086	0.051	0.947	35.268	−23.62
O1−X2_H(4) $-y+1,+x+1/2,+z-1/2$	2.4479	0.2853	0.1521	0.047	0.735	27.758	−19.103
O1−X1_H(7) $x,+y,+z-1$	2.8450	0.2230	−0.245	0.021	0.351	12.502	−7.615
O1−X1_H(8) $x,+y,+z-1$	2.8033	0.4001	−0.2033	0.020	0.340	12.068	−7.292
			B				
C2 X7_C(11) $-x+1/2,+y-1/2,-z+1/2$	3.6955	0.3020	−0.2256	0.039	0.359	14.409	−11.033
C2 X7_C(12) $-x+1/2,+y-1/2,-z+1/2$	3.5538	0.2951	−0.0837	0.053	0.499	20.736	−16.750
C3 X7_C(16) $-x+1/2,+y-1/2,-z+1/2$	3.6143	0.2789	−0.1443	0.043	0.393	15.983	−12.496
C3 X7_C(17) $-x+1/2,+y-1/2,-z+1/2$	3.6850	0.2800	−0.215	0.038	0.350	14.004	−10.668
C3 X7_C(21) $-x+1/2,+y-1/2,-z+1/2$	3.7365	0.3685	−0.2665	0.038	0.385	15.160	−11.246
C4 X1_C(14) $x,+y-1,+z$	3.7242	0.2216	−0.1842	0.034	0.334	13.062	−9.576
C6 X5_C(12) $x-1/2,+y-1/2,+z$	3.7965	0.0512	−0.3266	0.031	0.267	10.559	−7.891
C11 X7_C(19) $-x+1/2,+y-1/2,-z+1/2$	3.6280	0.2024	−0.088	0.037	0.319	12.874	−9.943
C11 X7_C(20) $-x+1/2,+y-1/2,-z+1/2$	3.7438	0.2945	−0.2037	0.036	0.372	14.520	−10.610
C6 X5_H(12) $x-1/2,+y-1/2,+z$	2.9132	0.1028	+0.0568	0.039	0.426	16.622	−12.139
C15 X3_H(14) $-x,-y+1,-z$	3.3756	0.3260	−0.292	0.016	0.187	6.754	−4.244
C20 X1_H(3B) $x,+y+1,+z$	3.7293	0.5152	−0.7592	0.004	0.107	3.591	−1.882
C22 X8_H(18) $x-1/2,-y+1/2,+z-1/2$	3.2946	0.3042	−0.3946	0.018	0.245	8.795	−5.453
C22 X8_H(19) $-x,+y-1,-z+1/2$	3.5546	0.2358	−0.6546	0.011	0.136	4.801	−2.865
C22 X6_H(22A) $-x-1/2,-y-1/2,-z$	3.5635	0.4181	−0.6635	0.010	0.151	5.251	−3.022
F1_X6_F(1) $-x+1/2,-y+1/2+1,-z$	2.6589	0.0055	0.3411	0.067	0.926	36.873	−27.869
O1_X1_H(14) $x,+y-1,+z$	2.5186	0.2884	0.0814	0.039	0.666	24.549	−16.102
O1_X1_H(15) $x,+y-1,+z$	2.9285	0.2385	−0.3285	0.017	0.272	9.623	−5.771
O1_X2_H(19) $-x,+y-1,-z+1/2$	2.6656	0.3800	−0.0656	0.024	0.495	17.485	−10.447
O1_X1_C(14) $x,+y-1,+z$	3.2264	0.1982	−0.0564	0.044	0.509	19.932	−14.646
O1_X1_C(15) $x,+y-1,+z$	3.4475	0.2249	−0.2775	0.025	0.285	10.629	−7.139
O1_X2_C(19) $-x,+y-1,-z+1/2$	3.5371	0.1811	−0.3671	0.027	0.298	11.225	−7.686

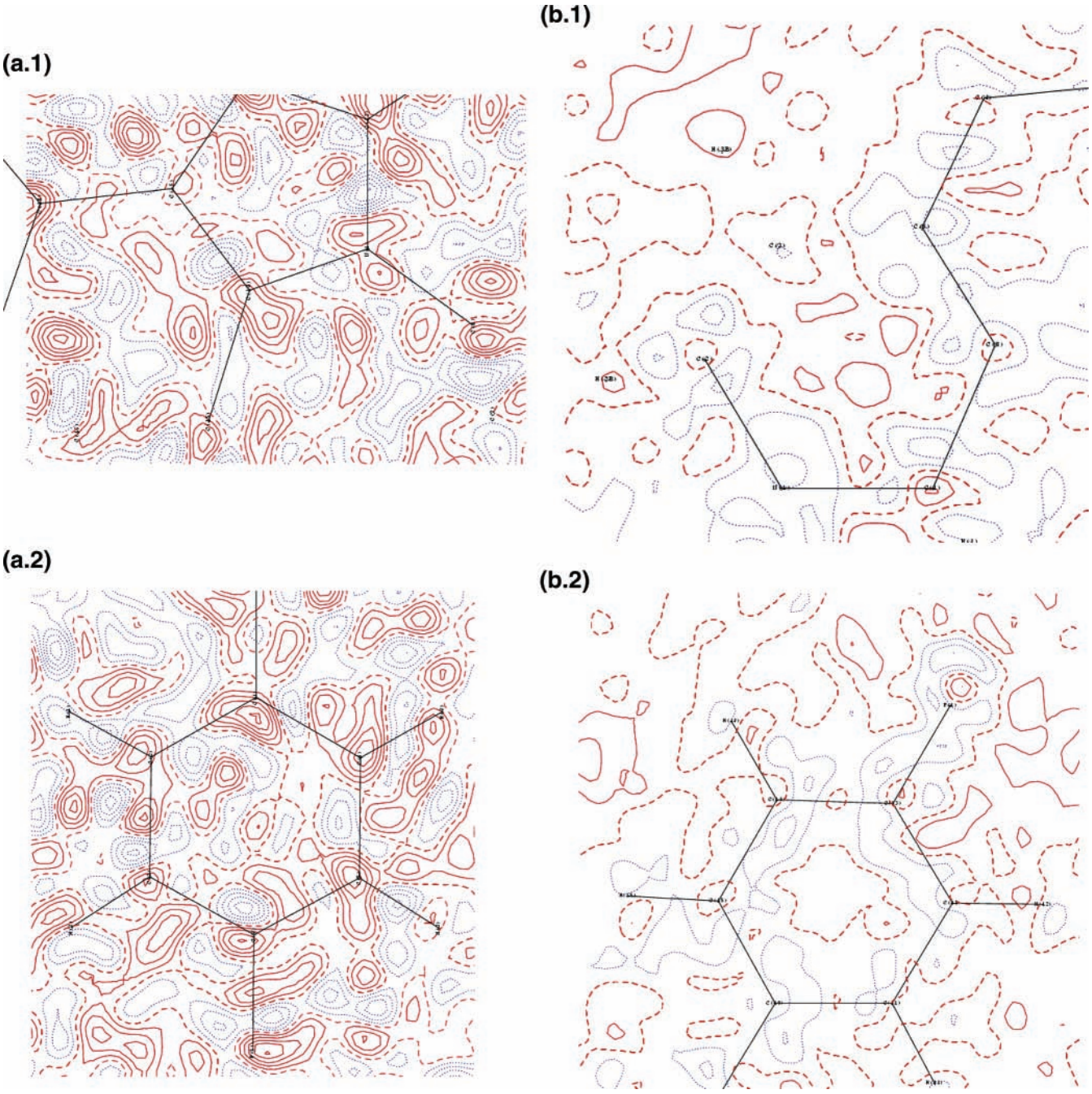

Figure 2. (a.1) Residual electron density in the molecular plane containing the fused ring junction. Contours are drawn at 0.05*e*/Å^3 intervals. Solid lines indicate positive contours, dotted lines indicate negative contours, and dashed red lines indicate zero contour. (a.2) Residual electron density in the molecular plane containing the fluorophenyl ring in compound **A**. Contours are drawn at 0.05*e*/Å^3 intervals. Solid lines indicate positive contours, and dotted lines indicate negative contours. The red dashed lines indicate zero contour. (b.1) Residual electron density in the molecular plane containing the fused ring junction in **B**. Contours are drawn at 0.05*e*/Å^3 intervals. Solid lines indicate positive contours, and blue dotted lines indicate negative contours. The red dashed lines indicate zero contour. (b.2) Residual electron density in the molecular plane containing the fluorophenyl ring in **B**. Contours are drawn at 0.05*e*/Å^3 intervals. Solid lines indicate positive contours, and blue dotted lines indicate negative contours. The red dashed lines indicate zero contour.

penetration of the hydrogen and the acceptor atom. This condition, considered as being necessary and sufficient, compares the nonbonded radii of the donor-hydrogen atom (r_D^0) and the acceptor atom (r_A^0) with their corresponding bonding radii. The nonbonding radius is taken to be equivalent to the gas phase van der Waals radius of the participating atoms.[39] The bonding radius (r) is the distance from the nucleus to the BCP. In a typical hydrogen bond, the values of $\Delta r_D = (r_D^0 - r_D) > \Delta r_A = (r_A^0 - r_A)$ and $\Delta r_D + \Delta r_A > 0$ represent positive interpenetration. If either or both of these conditions are violated, the interaction is essentially van der Waals in nature.

We have evaluated the nature of C−F···F−C interactions on the basis of the results obtained from experimental charge density analysis. The compounds studied are 1-(4-fluorophenyl)-3,6,6-trimethyl-2-phenyl-1,5,6,7-tetrahydro-4*H*-indol-4-one (**A**) and 1-(4-fluorophenyl)-6-methoxy-2-phenyl-1,2,3,4-tetrahydroisoquinoline (**B**) (see Scheme 1); the former has been used as a drug intermediate[40] in the industry. Interactions involving fluorine have been a subject of interest, and their presence to direct packing modes has been analyzed.[41] X-ray diffraction data at 113 K on compounds **A** and **B** have been subjected to multipole atom refinements followed by the AIM approach to

derive BCPs. It is of interest to note that compound **A** exhibits two polymorphic modifications[42] and in this study only the form that has the C−F···F−C contact has been subjected to charge density analysis.

Single-Crystal Data Collection and Spherical Refinement

High-resolution single-crystal X-ray diffraction data were collected on an AFC8/Saturn70 CCD diffractometer using Mo Kα radiation. During the data collection, the temperature was maintained at 113(3) K with a Rigaku X-Stream cooling system. A suitable crystal of reasonable size (Table 1) was mounted on the tip of a Lindeman glass (a tube gives much more rigidity to vibrations from the gas flow than a rod of a similar diameter, and a fine needle point of Lindeman glass greatly reduces any X-ray scatter from the mounting). It had been noted that, with a magnification of roughly 100 times, when the crystal was mounted on a glass fiber, it appeared to vibrate slightly under the cooling gas flow. This vibration was not visible when the crystal was mounted on top of a 1 mm capillary, when the top had been sealed and then pulled to a sharp point. The data were collected with 16 scans, each covering 180° in ω at 0.5°/frame at 120 s/deg (with $\chi = 0°$ and $\phi = 0, 180°$; $\chi = 45°$ and $\phi =$ 45, 90, 135, 180, 225, 270, 315°), for 2θ settings of 40 and 80°. The crystal-to-detector distance was fixed at 3.956 cm. This strategy provides completeness in the data sets up to 95% and covers all the reflections to the observable limit with an average redundancy of 4.46 and resolution of 0.45 Å [$(\sin\theta/\lambda)_{max} =$ 1.1 Å^{-1}]. The data collection was monitored and reduced with the package HKL2000.[43] Merging of the measured set of intensities was performed with SORTAV.[44] The structure was solved by a direct method using SHELXS97[45] and refined in the spherical atom approximation (based on F^2) using SHELXL97[45] included in the package, WinGX.[46] The molecular thermal ellipsoid plots are generated using ORTEP.[47]

Multipole Refinement

Multipole refinement of the data set was carried out with the module XDLSM incorporated in the software package XD.[48] Scattering factors were derived from the Clementi and Roetti[49] wave functions for all atoms. The function minimized in the least-squares refinement is $\sum w(|F_0|^2 - K|F_c|^2)^2$ for all reflections with $\boldsymbol{I} > 3\sigma(\boldsymbol{I})$. Initially, only the scale factor was refined with all reflections. Next, the higher order ($\sin\theta/\lambda \geq 0.8$ Å^{-1}) refinements were performed for position and anisotropic thermal parameters of the non-H atoms. The positional and isotropic thermal parameters of the H atoms were then refined using the lower angle data ($\sin\theta/\lambda \leq 0.8$ Å^{-1}). The positions of the H atoms in this refinement as well as in the subsequent refinements were fixed to average bond distance values obtained from reported[50] neutron diffraction studies (e.g., C−H = 1.085 Å). In the next stage of the refinements, monopole, dipole, quadrupole, and octapole populations (with a single κ value) were released in a stepwise manner. Finally, a single κ' value was refined for each species for all non-H atoms along with the rest of the parameters (including the isotropic thermal parameters of the H atoms). For all H atoms, the multipole expansion was truncated at the $l_{max} = 1$ (dipole, bond-directed) level. For each chemically different group of non-H atoms, separate κ and κ' values were allowed, while, for H atoms, the corresponding values were fixed at 1.2. No chemical restraints were applied, and the scale factor was allowed to refine. The modules XDFFT[48] and XDFOUR[48] were used to measure the amount of residual electron density and the dynamic deformation density

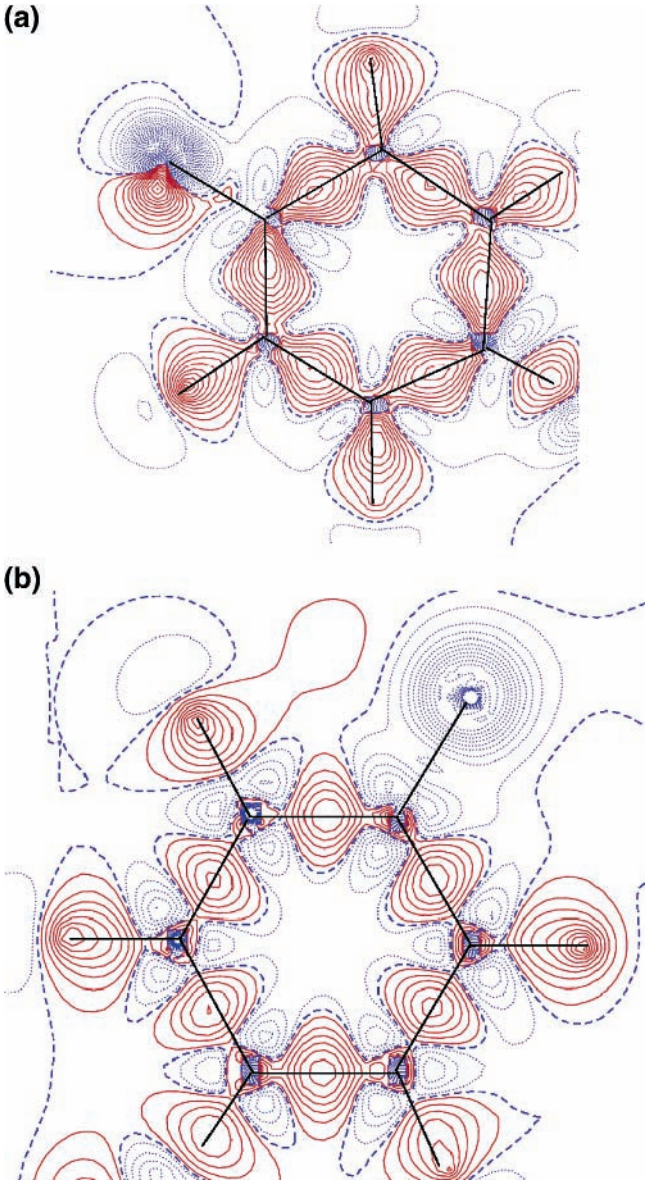

Figure 3. (a) Static experimental deformation density in the molecular plane containing the fluorophenyl ring in compound **A**. Contours are drawn at 0.1e/Å^3 intervals. The red solid lines indicate positive contours, the dotted blue lines indicate negative contours, and the dashed lines indicate zero contours. (b) Static experimental deformation density in the molecular plane containing the fluorophenyl ring in compound **B**. Contours are drawn at 0.1e/Å^3 intervals. The red solid lines indicate positive contours, the dotted blue lines indicate negative contours, and the dashed lines indicate zero contours.

and hence confirmed the refinement procedure. To get a quantitative description of the electronic structure, the module XDPROP[48] of the package XD was used for topological analysis of the charge densities.

Results and Discussion

The crystallographic details including unit cell parameters, the experimental aspects, R factors, and residual density values after the XD refinement for the two compounds are listed in Table 1. Figure 1 gives the ORTEP diagrams of the compounds showing the thermal ellipsoids at a 50% probability level along with the atom labeling. Table 2 lists the features of the intramolecular bond critical points for the two compounds, while the characteristic values for the intermolecular contacts are given

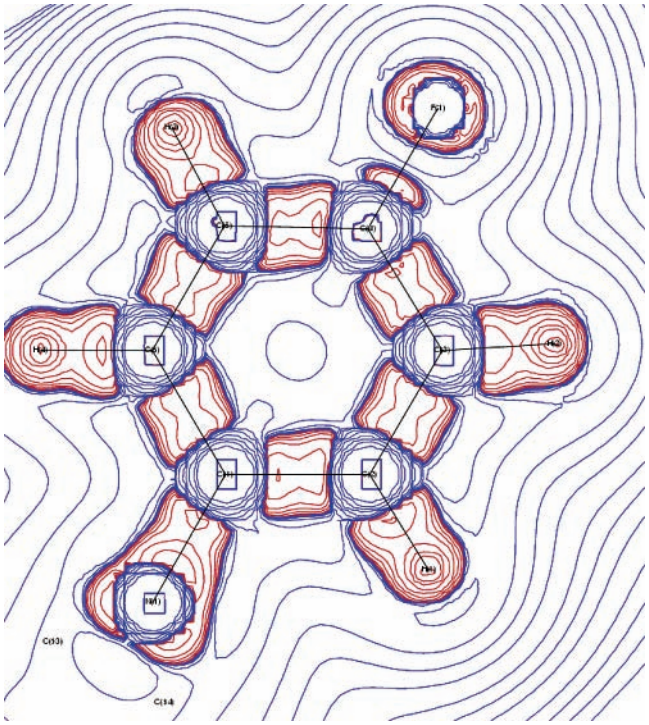

Figure 4. Negative Laplacian electron density distribution maps shown in the plane of the fluorophenyl ring in compound **A**. Contours are drawn at 0.1e/Å^3 intervals. The red and blue lines represent positive and negative contours, respectively.

in Table 3. The multipole population parameters ($P_{lm\pm}$ and P_v) along with κ and κ' from experimental refinements, local definition axes, fractional coordinates, thermal parameters, bond lengths, and bond angles are provided in theSupporting Information.

Charge Density Analysis of 1-(4-Fluorophenyl)-3,6,6-trimethyl-2-phenyl-1,5,6,7-tetrahydro-4*H*-indol-4-one (A)

In Hirshfeld's rigid bond test,[51] the largest differences of mean-square displacement amplitudes ($\Delta_{A,B}$) for **A** are 16 × 10^{-4} Å^2 for the bonds N(1)−C(1), N(1)−C(13), and N(1)−C(14), 12 × 10^{-4} and 13 × 10^{-4} Å^2 for the bond C(1)−C(2), and 16 × 10^{-4} Å^2 for the bond C(14)−C(15). The maximum residual peaks and hole after completion of the refinement were 0.355 and −0.417e/Å^3, respectively, and it is clear from the difference Fourier maps (Figure 2a), based on all available data, that there is no significant electron density that is not accounted by the model, a necessary condition for a successful multipole description. The static deformation density map representing only the fluorophenyl ring plane is given in Figure 3a. There is a lack of electron density in the C−F bond, a generally observed feature in molecules containing organic fluorine.[27,30] Figure 4 depicts the Laplacian in the region of the fluorophenyl moiety, and the topological analysis clearly brings out the covalent character of the C−F bond (Table 2). The value of the Laplacian at the observed (3, −1) critical point of the C (sp^2)−F bond is −23.05e/Å^5, which is typical for C−F bonds, as seen in the literature. For example, the value of the Laplacian was reported to be −15e/Å^5 in the structure of *p*-fluoromandelic acid,[25] −10.205e/Å^5 in the structure of 1,1-difluoroallene,[26] −20.0e/Å^5 in the complex of (*E*)-1,2-bis(4-pyridyl) ethylene with 1,4-diiodotetrafluorobenzene,[28] and −14.1e/Å^5 in tetrafluorophthalonitrile.[30]

It is of interest to note that the topological properties of the two C−N bonds of the five-membered indole ring differ, which clearly brings out the variation in charge density distribution at each nitrogen atom. Indeed, the N1−C13 bond has a considerably higher double bond character than the N1−C14 bond and the respective values for bond ellipticity are 0.33 and 0.02, respectively. Fluorine and nitrogen have a net charge of −0.046e

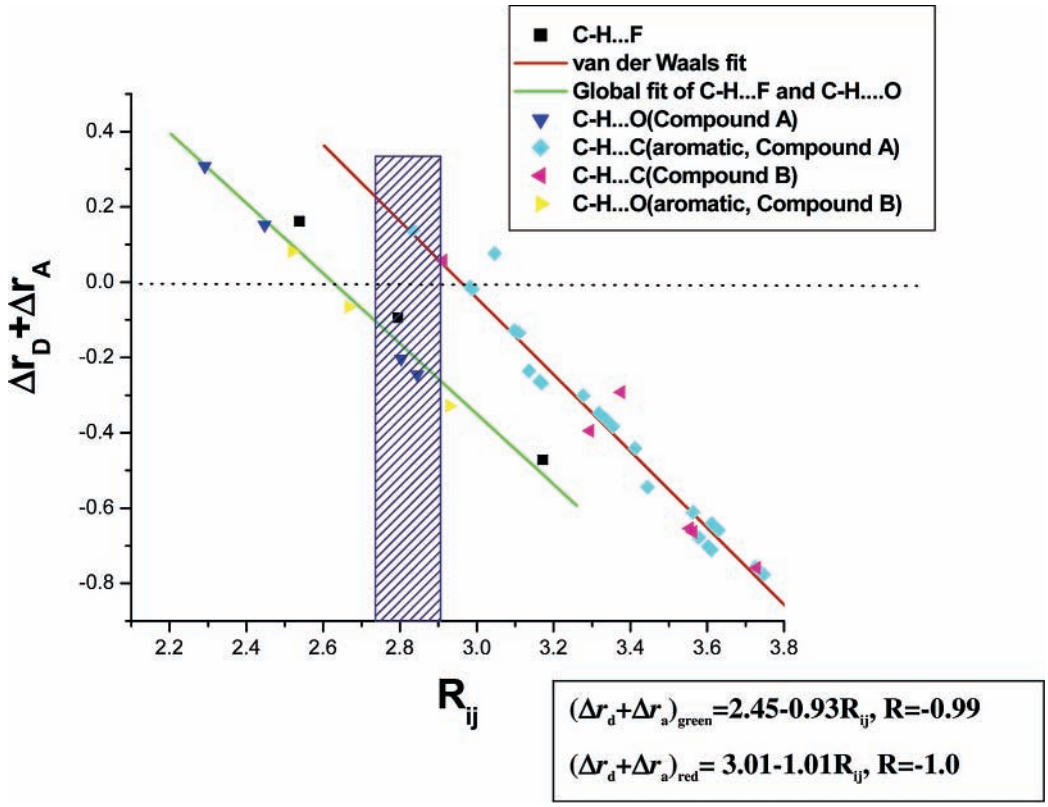

Figure 5. Linear dependence of ($\Delta r_D + \Delta r_A$) (Å) on R_{ij} (Å) for $N = 7$ (C−H···O), $N = 3$ (C−H···F), and $N = 32$ (C−H···π) points. The dotted line corresponds to ($\Delta r_D + \Delta r_A$) = 0. The hatched area represents the region of overlap as defined in ref 1.

TABLE 4: Intermolecular Bond Critical Points and Topological Parameters Characterizing the C−F···F Contacts and C−H···F Interactions (Pilati et al.[28])

compound	R_{ij}	ρ_b	$\nabla^2\rho_b$	$G(r_{CP})$	$V(r_{CP})$	$E(r_{CP})$	$\Delta r_D + \Delta r_A$
A[a]	2.8091	0.049	1.030	37.752	−24.476	13.276	0.1309
B[b]	2.659	0.067	0.926	36.873	−27.869	9.003	0.2811
Hursthouse[c]	2.899	0.040	0.700	25.782	−16.884	8.898	0.041
	2.862	0.050	0.820	30.944	−21.264	9.680	0.086
	2.862	0.040	0.800	29.084	−18.535	10.549	0.086
	3.063	0.030	0.500	18.162	−11.553	6.609	−0.123
	3.198	0.020	0.400	14.05	−8.283	5.767	−0.258
Pilati[d]	3.033	0.034	0.600	21.847	−13.969	7.878	−0.093
PFBA[e]	2.627	0.058	1.233	45.668	−30.251	15.417	0.3131
	2.628	0.067	1.410	52.858	−35.862	16.996	0.3120

C−H···F	R_{ij}	ρ_b	$\nabla^2\rho_b$	$G(r_{CP})$	$V(r_{CP})$	$E(r_{CP})$	$r_D + \Delta r_A$
f	2.44	0.071	1.09	42.927	−31.854	11.073	0.230
g	2.90	0.024	0.38	13.687	−8.548	5.139	−0.230
h	2.49	0.030	0.66	23.447	−14.195	9.251	0.180
i	2.74	0.03	0.50	18.162	−11.553	6.609	−0.070

[a] Symmetry code: $-x+1/2+1, y+1/2+1, +z$. [b] Symmetry code: $-x-1/2, -y-1/2, -z$. [c] Symmetry code: $-x, y+1/2, -z+1/2$; $x-1/2, y, -z+1/2$; $-x+1/2, -y-1/2, -z+1$; $-x+1/2, -y, z-1/2$; $x+1/2, -y-1/2, -z+1$. [d] Symmetry code: $-x-1, -y, -z$. [e] Symmetry code: $-x+2, -y, -z+1$; $-x+2, -y, -z$. [f] C−H···F (Pilati et al.[28]): $x+1, y, z$. [g] C−H···F (Pilati et al.[28]): $-x, -y+1, -z-1$. [h] C−H···F (Pilati et al.[28]): $x-1, y, z+1$. [i] C−H···F (Pilati et al.[28]): $x-1, y, z+1$.

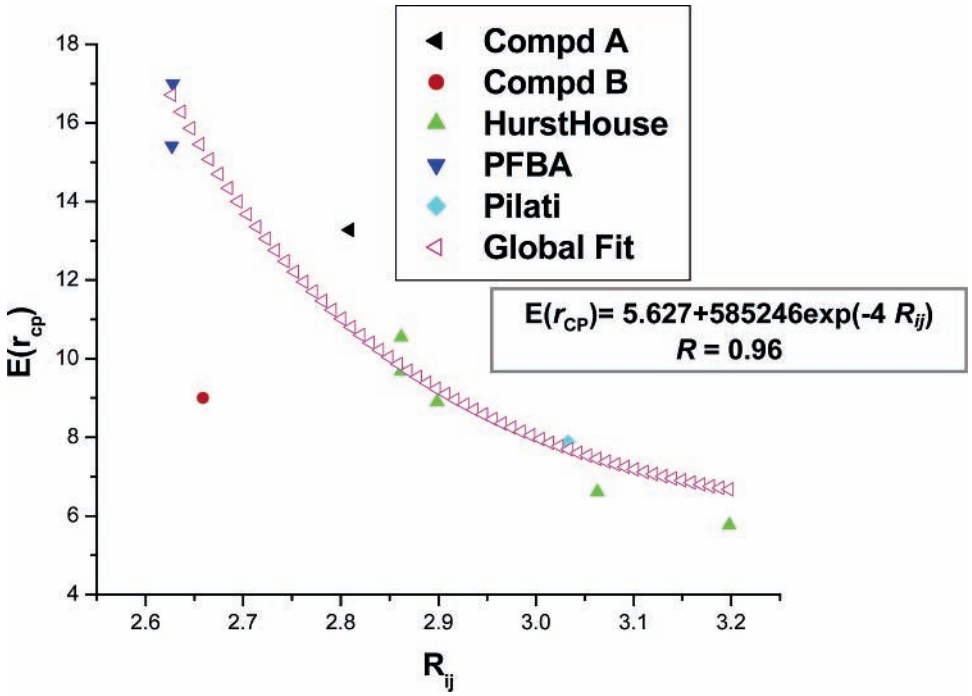

Figure 6. Exponential dependence of total energy density ($E(r_{CP})$) (kJ mol^{-1} bohr^{-3}) on R_{ij} (Å) for $N = 10$ data points. The inset gives the details of the fitting models along with correlation coefficients (R).

and +0.066*e*, whereas oxygen has a net negative charge of −0.278*e*, suggesting a higher propensity for H-bond formation involving the oxygen atom. The oxygen atom, in fact, forms two intermolecular C−H···O hydrogen bonds, one with the carbon atom C2 and the other with C6. These intermolecular interactions obey all four conditions (Table 3) required to form a hydrogen bond on the basis of the Koch and Popelier criteria. Table 3 also gives the features of the two other C−H···F intermolecular interactions as well as that of one $C-F^{\delta-}\cdots F^{\delta-}-C$ short contact [interaction length R_{ij} = 2.809(3) Å < sum of the van der Waals radius of 2.94 Å, with a characteristic (3, −1) critical point; Table 3], generating the packing features across the 4_2 screw axis in the crystal lattice. Interestingly, this interaction length is just about twice the fluorine radius worked out by Nyburg and Faerman[39] on the basis of a CSD analysis considering the effect of flattening along the C−F bond and the negative charge carried by the fluorine atom. Further, the charge density at the critical point in the C−F···F−C interaction is +0.049*e*/Å^3 and the corresponding value of the Laplacian is +1.03*e*/Å^5, a clear indication of a closed-shell interaction. Such features have also been observed in interactions of the type $C-H^{\delta+}\cdots H^{\delta+}-C$ which suggested closed-shell stabilizing interactions can occur between two hydrogen atoms of similar charge.[52,53]

Charge Density Analysis of 1-(4-Fluorophenyl)-6-methoxy-2-phenyl-1,2,3,4-tetrahydroisoquinoline (B)

The chemical bonds in this structure were initially tested to ascertain whether Hirshfield's rigid bond criterion[51] is satisfied. The largest differences of mean-square displacement amplitudes ($\Delta_{A,B}$) observed for N(1)−C(16) and N(1)−C(2) are 10×10^{-4}

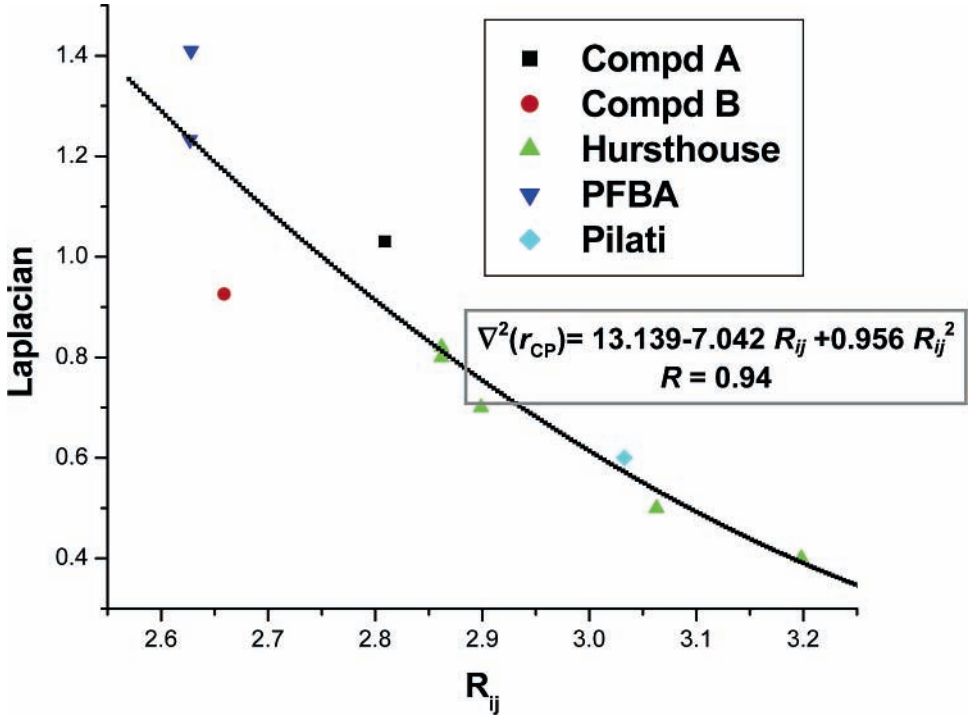

Figure 7. Morse-like dependence of the Laplacian $\nabla^2(r_{CP})$ (e/Å^5) on R_{ij} (Å) for $N = 10$ data points.

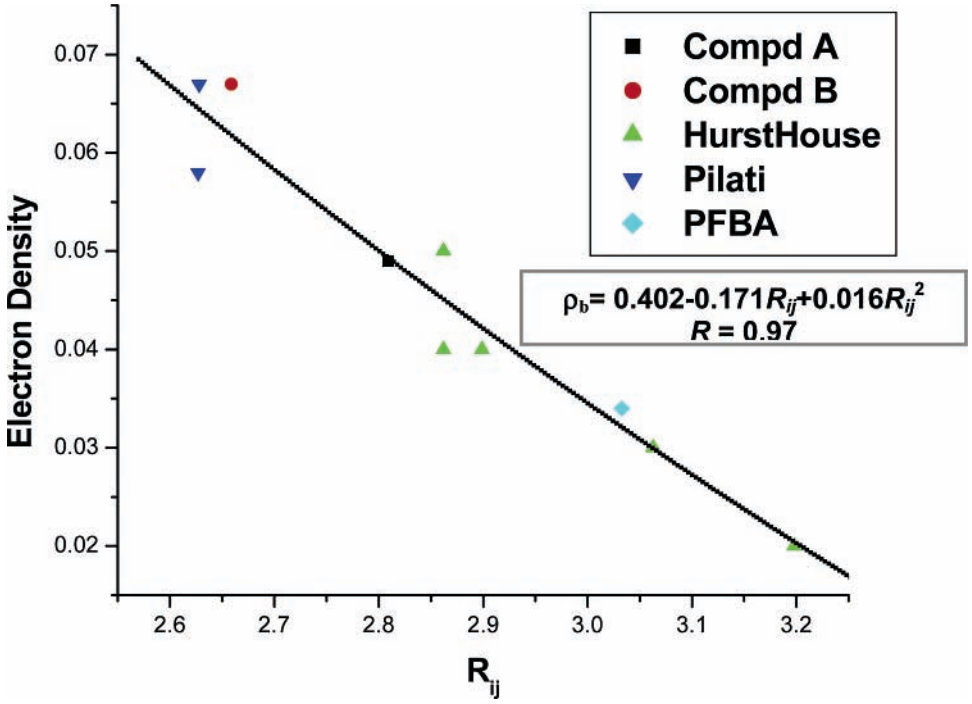

Figure 8. Quadratic dependence of the electron density (ρ_b) at the critical point with the interaction length (R_{ij}) for $N = 10$ data points.

and 13×10^{-4} Å^2, respectively. The maximum residual peak and hole after completion of the refinement was 0.170 and $-0.192e$/Å^3. The difference Fourier maps representing the isoquinoline and the fluorophenyl ring indicate that the electron density has been modeled satisfactorily (Figure 2b). The static deformation density map representing only the fluorophenyl ring plane is given in Figure 3b. The value of the Laplacian at the observed (3, −1) critical point of the C (sp^2)−F bond is $-7.21(8)e$/Å^5 which is comparable to the literature value of $-6.5(3)e$/Å^5 reported in the case of tetrafluoroisophthalonitrile.[30] As compared to the values of the Laplacian in **A**, this value appears to reduce the covalency in the C−F bond. It is of interest to note that the topological properties of the two C−O bonds are different, with the ellipticities being 0.11 and 0.28, respectively, indicating differences in the electronic environment around the oxygen atom. Compared to compound **A**, the fluorine atom possesses a net positive charge of $+0.882e$, with the corresponding charges on oxygen and nitrogen being $0.529e$ and $0.224e$, respectively. There are three C−H···O intermolecular contacts with H···O distances less than 2.95 Å of which only one involving hydrogen H14 (Table 3) satisfies all four Koch and Popelier criteria for the formation of a hydrogen bond. It is noteworthy that a short C−$F^{\delta+}$···$F^{\delta+}$−C contact across the center of symmetry with an interaction length of 2.659

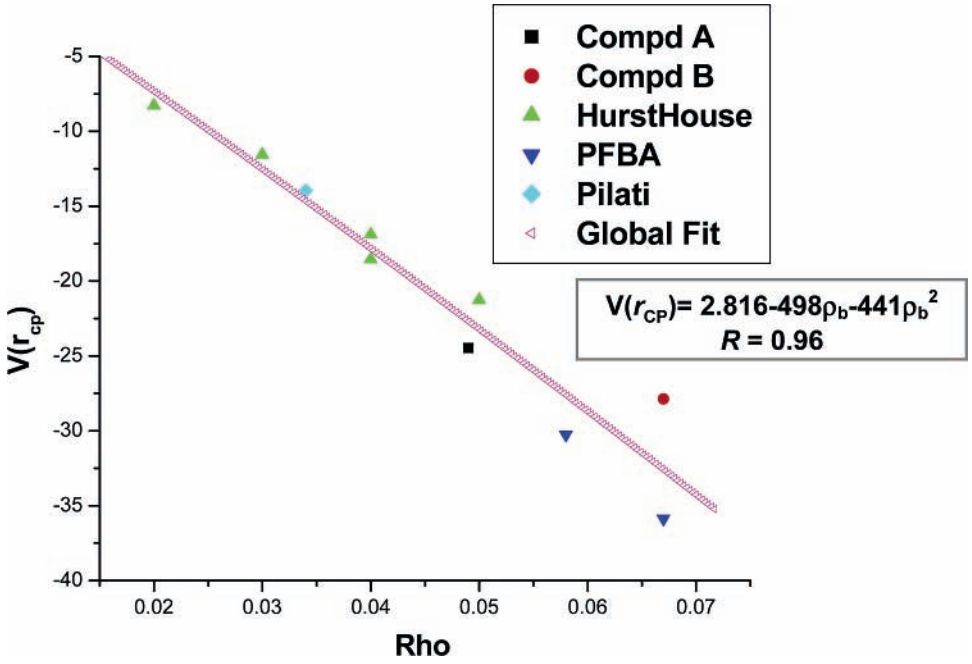

Figure 9. Quadratic relationship between local potential energy density ($V(r_{CP})$) (kJ mol^{-1} bohr^{-3}) and ρ_b (e/Å^3) for $N = 10$ data points.

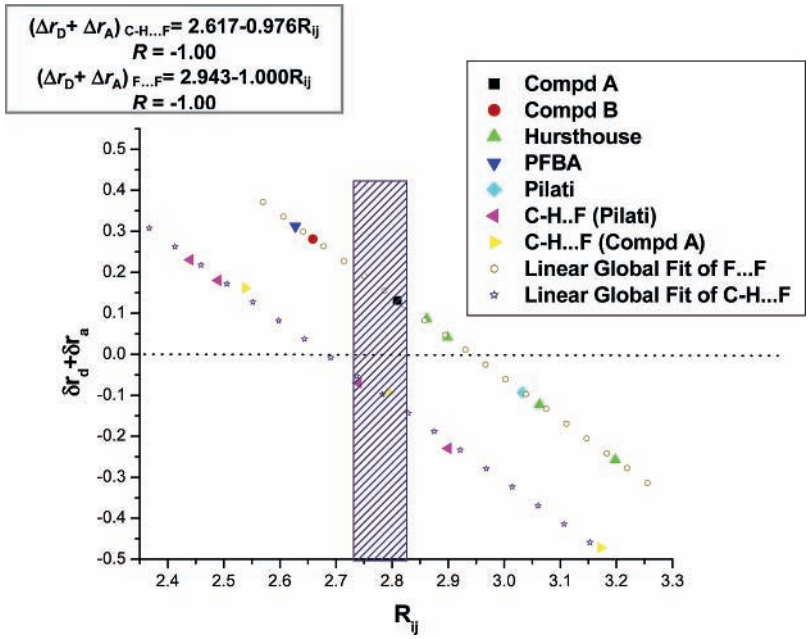

Figure 10. Linear dependence of ($\Delta r_D + \Delta r_A$) (Å) with R_{ij} (Å) for $N = 10$ points for C−F···F−C contacts and $N = 7$ points for C−H···F interactions.

Å is observed in the crystalline lattice. Further, the value of the charge density at the critical point in the C−F···F−C interaction is $+0.067e$/Å^3 and the corresponding value of the Laplacian is $+0.93e$/Å^5. Thus, even though the charge carried by the fluorine atom is positive in **B** and negative in **A**, the characteristic values of the density and the Laplacian at the critical point represent a closed-shell interaction similar to those observed in the C−H$^{\delta+}$···H$^{\delta+}$−C contacts.

Classification of Intermolecular Interactions Based on Koch and Popelier Criteria

Both molecules provide an opportunity to evaluate the features of weak interactions such as C−H···O hydrogen bonds, C−H···π interactions, C−H···F interactions, and the C−F···F−C short contacts in terms of the first four criteria suggested by Koch and Popelier on the basis of the topological analysis in the AIM framework. There are 4 C−H···O hydrogen bonds, 26 C−H···π interactions, 3 C−H···F interactions, and 1 C−F···F−C interaction in structure **A**, whereas 3 C−H···O hydrogen bonds, 6 C−H···π interactions, no C−H···F interactions, and 1 C−F···F−C interaction pack the molecules in structure **B**. All of these contacts have been subjected to test the first four criteria. Correlation plots characterizing the first three criteria are available in the Supporting Information. In accordance with the fourth criterion, the generally observed linear correlation between $\Delta r_D + \Delta r_A$ and R_{ij} is found (Figure 5). It is seen that all seven C−H···O contacts lie in the hydrogen bonding regime[1] and almost all C−H···π contacts are in the van der Waals region with a few lying in the region of overlap (Figure 5). The C−H···F contacts are more hydrogen bond like

than van der Waals ones and display characteristics of a weak hydrogen bond. It is of interest to note that the C−H···F interactions correspond to an interaction energy density of −17.75 kJ mol^{-1} bohr^{-3}, which is comparable to that shown by a C−H···O hydrogen bond (−19.1 kJ mol^{-1} bohr^{-3}, Table 3).

Features of C−F···F−C Contacts

The two structures subjected to charge density studies as above offer a unique platform to study the ubiquitous F···F intermolecular contacts involving organic fluorine. It is clear from the above studies and also from literature[27,28,30] that the F···F intermolecular contacts exhibit all the required features of closed-shell interactions. Further, from the topological analysis, there is a well-defined bond path with a critical point (generally coincident with a symmetry element of the unit cell) along the F···F direction. In a recent article, Matta, Castillo, and Boyd[54] elaborated on the F···F contacts in the intramolecular regime of a large number of aromatic compounds and have concluded on the basis of the theory of AIM that F···F bonding occurs in polyfluorinated aromatic compounds with an internuclear separation of 2.3−2.8 Å. Further, they conclude that the electron density at the critical point decreases with distance and the interaction is a typical closed-shell interaction in terms of the topological properties such as the Laplacian and energy densities. They also mention that such a contact imparts as much as 14 kcal/mol of local stabilization to the molecule.

The F···F intermolecular contacts identified in the two compounds, **A** and **B**, along with the ones reported in the literature[27,28,30] show similar trends to those observed among the F···F intramolecular contacts. Figures 6−10 and Table 4 show the correlations in the derived properties suggesting that these contacts do provide stability in the context of crystal packing like those shown by H···H bonding.[52,53] The energy plot (Figure 6) suggests that, with an increase in internuclear distance, R_{ij}, the energy density shows trends of decrease in energy at the bond critical point (BCP). This feature is common in a variety of intermolecular contacts,[1] thus classifying the F···F contact as a well-defined intermolecular interaction. The remaining correlation plots (Figures 7−9) show features akin to the observations made for F···F intramolecular bonds.[54] Indeed, Figure 10 clearly points out that the F···F contacts belong to the general regime of other weak intermolecular interactions with altered penetration of van der Waals spheres in C−H···F and F···F contacts.

Conclusions

The comparative study of intermolecular interactions involving organic fluorine in aromatic compounds via experimental charge density analysis using the AIM approach has sorted out the ubiquitous nature of F···F contacts in molecular crystals. The first four criteria proposed by Koch and Popelier followed by the analysis with respect to the approach followed by our earlier analysis[1] have led to a clear characterization of such contacts and have established the hierarchy in weak intermolecular interactions.

Acknowledgment. We are thankful to Dr. A. R. Choudhury for giving crystals of compound **B**. We thank Department of Science and Technology [DST0611], India, for financial support, and D.C. thanks CSIR, India, for the award of a junior research fellowship. We thank Rigaku/MSC for the provision of data collection facilities, and T.S.C. thanks NSERC for financial support.

Supporting Information Available: Fractional atomic coordinates, anisotropic thermal parameters, bond lengths and angles, torsion angles, multipole population coefficients, κ and κ' values obtained from the multipole refinement, and definition of local axes. Figures S1−S5 depict the experimental correlations observed for the first three criteria of Koch and Popelier. This material is available free of charge via the Internet at http://pubs.acs.org.

References and Notes

(1) (a) Munshi, P.; Guru Row, T. N. *J. Phys. Chem. A* **2005**, *109*, 659−672. (b) Munshi, P.; Guru Row, T. N. *CrystEngComm* **2005**, *7*, 608−611.

(2) Bader, R. F. W. *Atoms in Molecules: A Quantum Theory*; Oxford University Press: Oxford, U.K., 1990.

(3) Bader, R. F. W. *J. Phys. Chem. A* **1998**, *102*, 7314−7323.

(4) (a) Desiraju, G. R. *Acc. Chem. Res.* **1991**, *24*, 290−296. (b) Aakeroy, C. B.; Sneddon, K. R. *Chem. Soc. Rev.* **1993**, *22*, 397−407. (c) Desiraju, G.; Kashino, S.: Coombs, M. M.: Glusker, J. *Acta Crystallogr.* **1993**, *B49*, 880−892.

(5) Steiner, T. *Crystallogr. Rev.* **2003**, *9* (2−3), 177−228.

(6) (a) Umezawa, Y.; Tsuboyama, S.; Honda, K.; Uzawa, J.; Nishio, M. *Bull. Chem. Soc. Jpn.* **1998**, *71*, 1207−1213. (b) Umezawa, Y.; Tsuboyama, S.; Takahashi, H.; Uzawa, J.; Nishio, M. *Tetrahedron* **1999**, *55*, 10047−10056.

(7) Nishio, M.; Hirota, M.; Umezawa, Y. *The CH/pi Interaction. Evidence, Nature, and Consequences*; Wiley-VCH: New York, 1998.

(8) Nishio, M. *CrystEngComm* **2004**, *6* (27), 130−158.

(9) Mallinson, P. R.; Woz′niak, K.; Wilson, C. C.; McCormac, K. L. Yufit, D. S. *J. Am. Chem. Soc.* **1999**, *121*, 4640−4646.

(10) Ellena, J.; Goeat, A. E.; Howard, J. A. K.; Punte, G. *J. Phys. Chem. A* **2001**, *105*, 8696−8708 and references therein.

(11) Oddershede, J.; Larsen, S. *J. Phys. Chem. A* **2004**, *108*, 1057−1063.

(12) Murray-Rust, P.; Stallings, W. C.; Monti, C. T.; Preston, R. K.; Glusker, J. P. *J. Am. Chem. Soc.* **1983**, *105*, 3206−3214.

(13) Sarma, J. A. R. P.; Desiraju, G. R. *Acc. Chem. Res.* **1986**, *19*, 222−228.

(14) Price, S. L.; Stone, A. J.; Rowland, R. S.; Thornley, A. E. *J. Am. Chem. Soc.* **1994**, *116*, 4910−4918.

(15) Ramasubbu, N.; Parthasarathy, R.; Murray-Rust, P. *J. Am. Chem. Soc.* **1986**, *108*, 4308−4314.

(16) Desiraju, G.; Parthasarathy, R. *J. Am. Chem. Soc.* **1989**, *111*, 8725−8726.

(17) Shimoni, L.; Carell, H. L.; Glusker, J. P.; Coombs, M. M. *J. Am. Chem. Soc.* **1994**, *116*, 8162−8168.

(18) Pauling, L. *The Nature of the Chemical Bond*, 3rd ed.; Cornell University Press: Ithaca, NY, 1960.

(19) Tsirelson, V.; Zou, P. F.; Tang, T.-H.; Bader, R. F. W. *Acta Crystallogr., Sect. A* **1995**, *51*, 143−153.

(20) (a) Shimoni, L.; Glusker, J. P. *Struct. Chem.* **1994**, *5*, 383−397. (b) Howard, J. A. K.; Hoy, V. J.; O'Hagan D.; Smith, G. *Tetrahedron* **1996**, *52*, 12613−12622. (c) Duntiz, J. D.; Taylor, R. *Chem.—Eur. J.* **1997**, *3*, 89−98. (d) Haufe, G.; Rossen, T. C.; Meyer, O. G. J.; Frohlich, R., Rissanen, K. *J. Fluor. Chem.* **2002**, *114*, 4253−4264. (d) Dunitz, J. D. *ChemBioChem* **2004**, *5*, 614−621.

(21) Buschmann, J.; Koritsanszky, T.; Kuschel, R.; Luger. P.; Seppelt, K. *J. Am. Chem. Soc.* **1991**, *113*, 233−238.

(22) Kuboto, M.; Ohba, S. *Acta Crystallogr., Sect. B* **1992**, *48*, 849−854.

(23) Irngartinger, H.; Shack, S. *J. Am. Chem. Soc.* **1998**, *120*, 5818−5819.

(24) Mallinson, P. R.; Barr, G.; Coles, S. J.; Guru Row, T. N.; MacNicol, D. D.; Teat, S. J.; Wozniak, K. *J. Synchrotron Radiat.* **2000**, *7*, 160−166.

(25) Larsen, S.; Flensburg, C.; Bengacted, H. S.; Sorenson, H. O. *Acta Crystallogr., AS55*, **1999**, 38.

(26) Buschmann, J.; Koritsanszky, T.; Lentz, D.; Luger, P.; Nickelt, N.; Willemsen, S. *Z. Kristallogr.* **2000**, *215*, 487.

(27) Bach, A.; Lentz, D.; Luger, P *J. Phys. Chem. A* **2001**, *105*, 7405−7412.

(28) Bianchi, R.; Forni, A.; Pilati, T. *Chem.—Eur. J.* **2003**, *9*, 1631−1638.

(29) (a) Choudhury A. R.; Guru Row, T. N. *Cryst. Growth Des.* **2004**, *4*, 47−52. (b) Choudhury A. R.; Guru Row, T. N. *CrystEngComm* **2006**, *8*, 265−274.

(30) Hibbs, D. E.; Overgaard, J.; Platts, J. A.; Waller, M. P.; Hursthouse, M. B. *J. Phys. Chem. B* **2004**, *108*, 3663−3672.

(31) Coppens, P. *Acta Crystallogr.* **1998**, *A54*, 779−788.

(32) Coppens, P. *X-ray Charge Densities and Chemical Bonding*; Oxford University Press: Oxford, U.K., 1997.

(33) Koritsanszky, T. S.; Coppens, P. *Chem. Rev.* **2001**, *101* (6), 1583−1621.

(34) Hansen, N. K., Coppens, P. *Acta Crystallogr*. **1978**, *A34*, 909−921.

(35) Koch, U.; Popelier, P. L. A. *J. Phys. Chem.* **1995**, *99*, 9747−9754.

(36) Popelier, P. *Atoms in Molecules. An Introduction*; Prentice Hall: Harlow, U.K., 2000; pp 150−153.

(37) Abramov, Yu. A. *Acta Crystallogr*. **1997**, *A53*, 264−272.

(38) Espinosa, E.; Molins, E.; Lecomte, C. *Chem. Phys. Lett.* **1998**, *285*, 170−173.

(39) (a) Bondi, A. *J. Phys. Chem.* **1964**, *68*, 441−451. (b) Nyburg, S. C.; Faerman, C. H. *Acta Crystallogr.* **1985**, *B41*, 274−279.

(40) Nagarajan, K.; Tawalker, P. K.; Shah, R. K., Mehta, S. R.; Nayak, G. V. *Ind. J. Chem*. **1985**, *24b*, 98−111.

(41) Chopra, D.; Guru Row, T. N. *J. Mol. Struct.* **2005**, *733*, 133−141.

(42) Chopra, D.; Nagarajan K.; Guru Row, T. N. *Cryst. Growth Des*. **2005**, *5*, 1035−1039.

(43) Otwinowski, Z.; Minor, W. Processing of X-ray Diffraction Data Collected in Oscillation Mode. In *Macromolecular Crystallography*. *Part A*; Carter, C. W., Jr., Sweet, R. M., Eds.; Methods in Enzymology, Vol. 276; Academic Press: San Diego, CA, 1997; pp 307−326.

(44) Blessing, R. H. *Crystallogr. Rev.* **1987**, *1*, 3−58.

(45) Sheldrick, G. M. *SHELXS97* and *SHELXL97*; University of Göttingen: Göttingen, Germany, 1997.

(46) Farrugia, L. J. *J. Appl. Crystallogr.* **1999**, *32*, 837−838 (WinGX, version 1.64.05).

(47) Farrugia, L. J. *J. Appl. Crystallogr.* **1997**, *30*, 565 (ORTEP-3).

(48) Koritsanszky, T. S.; Howard, S.; Macchi, P.; Gatti, C.; Farrugia, L. J.; Mallinson, P. R.; Volkov, A.; Su, Z.; Richter, T.; Hansen, N. K. *XD, A computer program package for multipole refinement and analysis of electron densities from diffraction data*, version 4.10, July; Free University of Berlin, Germany; University of Wales, Cardiff, U.K.; Università di Milano, U.K.; CNR-ISTM, Milano, U.K.; University of Glasgow, U.K.; State University of New York, Buffalo, NY; University of Nancy, France, 2003.

(49) Clementi, E.; Roetti, C. *At. Data Nucl. Data Tables* **1974**, *14*, 177.

(50) Allen, F. H.; *Acta Crystallogr.* **1986**, *B42*, 515−522.

(51) Hirshfeld, F. L. *Acta Crystallogr.* **1976**, *A32*, 239−244.

(52) Matta, C. F. In *Hydrogen Bonding—New Insight*; Grabowski, S., Ed.; Challenges and Advances in Computational Chemistry and Physics Series; Kluwer: New York, 2006.

(53) Matta, C. F.; Hernandez-Trujillo, J.; Tang, T. H.; Bader, R. F. W. *Chem.—Eur. J.* **2003**, *9*, 1940−1951.

(54) Matta, C. F.; Castillo, N.; Boyd, R. J. *J. Phys. Chem. A* **2005**, *109*, 3669−3681.